J Appl Physiol 97: 1486–1495, 2004;
10.1152/japplphysiol.00378.2004.

Cannabinoid receptor expression in peripheral arterial chemoreceptors during postnatal development

Gabrielle L. McLemore,[1] Reed Z. B. Cooper,[2] Kimberlei A. Richardson,[2] Ariel V. Mason,[2] Cathleen Marshall,[2] Frances J. Northington,[2] and Estelle B. Gauda[2]

[1]*Department of Biology, School of Computer, Mathematical, and Natural Sciences, Morgan State University, Baltimore 21251; and* [2]*Department of Pediatrics, Division of Neonatology, Johns Hopkins Medical Institutions, Baltimore, Maryland 21287-3200*

Submitted 7 April 2004; accepted in final form 21 May 2004

McLemore, Gabrielle L., Reed Z. B. Cooper, Kimberlei A. Richardson, Ariel V. Mason, Cathleen Marshall, Frances J. Northington, and Estelle B. Gauda. Cannabinoid receptor expression in peripheral arterial chemoreceptors during postnatal development. *J Appl Physiol* 97: 1486–1495, 2004; 10.1152/japplphysiol.00378.2004.—Prenatal exposure to tobacco smoke increases risk of sudden infant death syndrome (SIDS). Marijuana is frequently smoked in conjunction with tobacco, and perinatal exposure to marijuana is associated with increased incidence of SIDS. Abnormalities in peripheral arterial chemoreceptor responses during sleep may be operative in infants at risk for SIDS, and nicotine exposure adversely affects peripheral arterial chemoreceptor responses. To determine whether marijuana could potentially affect the activity of peripheral arterial chemoreceptors during early postnatal development, we used in situ hybridization histochemistry to characterize the pattern and level of mRNA expression for cannabinoid type 1 receptor (CB1R) in the carotid body, superior cervical ganglia (SCG), and nodose-petrosal-jugular ganglia (NG-PG-JG) complex in newborn rats. We used immunohistochemistry and light, confocal, and electron microscopy to characterize the pattern of CB1R and tyrosine hydroxylase protein expression. CB1R mRNA expression was intense in the NG-PG-JG complex, low to moderate in the SCG, and sparse in the carotid body. With maturation, CB1R gene expression significantly increased ($P < 0.01$) in the NG-PG-JG complex. CB1R immunoreactivity was localized to nuclei of ganglion cells in the SCG and NG-PG-JG complex, whereas tyrosine hydroxylase immunoreactivity was localized to the cytoplasm. Exposure to marijuana during early development could potentially modify cardiorespiratory responses via peripheral arterial chemoreceptors. The novel finding of nuclear localization of CB1Rs in peripheral ganglion cells suggests that these receptors may have an, as yet, undetermined role in nuclear signaling in sensory and autonomic neurons.

nodose-petrosal-jugular ganglia; superior cervical ganglion; carotid body; in situ hybridization histochemistry; immunohistochemistry

PERINATAL EXPOSURE TO TOBACCO smoke is the leading modifiable risk factor for sudden infant death syndrome (SIDS) (14, 28). Infants exposed to maternal tobacco smoke frequently have depressed hypoxic arousal responses, reduced respiratory drive, and blunted ventilatory responses to hypoxia, all of which may be caused by abnormalities of peripheral arterial chemoreceptor function. Peripheral arterial chemoreceptors in the carotid body contain neuromodulators that bind G protein-coupled receptors (GPCRs) (15, 36), which modulate respiratory responses to hypoxia (23) and the level of arousal from sleep (10). Marijuana, the most widely consumed illicit drug during pregnancy (7, 9), is frequently smoked with tobacco (48). Marijuana has been associated with intrauterine growth retardation, dysmorphic features, behavioral abnormalities during the neonatal period, abnormalities in psychomotor and cognitive development (22), and abnormal arousal from sleep (10).

The physiological effects of Δ^9-tetrahydrocannabinol (THC), the psychoactive component of marijuana, as well as endogenous cannabinoids ("endocannabinoids"), are mediated through two distinct types of GPCRs: cannabinoid type 1 (CB1R) and type 2 (CB2R) receptors. CB1Rs are most abundant in the brain (45) and peripheral nervous system (PNS) (13, 26), and CB2Rs are found in immune tissues (31, 34). In the PNS, the binding of endogenous cannabinoids or THC to CB1Rs regulates neurotransmission in autonomic and sensory neurons, which modify cardiovascular responses (38). Furthermore, endogenous and exogenous cannabinoids modulate the level of arousal from sleep in adult rats (4) and induce sympathoinhibition by reducing plasma norepinephrine levels and enhancing vagal tone (32). Reduced arousal from sleep (19) and altered vagal tone are mechanisms that may contribute to SIDS (11). Maternal (42) and paternal (21) marijuana use during conception, pregnancy, and infancy is associated with an increased risk of SIDS. Because peripheral arterial chemoreceptors are key modulators of arousal from sleep and cardiorespiratory responses in the newborn and because cannabinoids modulate peripheral arterial chemoreceptor function, we used in situ hybridization histochemistry (ISHH), immunohistochemistry (IHC), and light, confocal, and electron microscopy to characterize and localize gene and protein expression of CB1Rs in the carotid body, superior cervical ganglia (SCG), and nodose-petrosal-jugular ganglia (NG-PG-JG) complex of newborn rats during the 1st mo of postnatal development to determine whether exogenous and endogenous cannabinoids could potentially modify peripheral arterial chemoreceptor activity.

METHODS

ISHH

Sprague-Dawley rats were used in experimental protocols approved by the Animal Care and Use Committee at Johns Hopkins University. The animals were deeply anesthetized with halothane and immediately decapitated. Tissues were removed from animals at *days of life* (*DOL*) *5, 7,* and *14* and processed for ISHH. The right and left

Address for reprint requests and other correspondence: G. L. McLemore, Dept. of Biology, Morgan State Univ., 1700 East Cold Spring Ln., Baltimore, MD 21251 (E-mail: McLemoreGLynn@yahoo.com).

The costs of publication of this article were defrayed in part by the payment of page charges. The article must therefore be hereby marked "*advertisement*" in accordance with 18 U.S.C. Section 1734 solely to indicate this fact.

bifurcation of the carotid artery, including the carotid body, SCG, and NG-PG-JG complex were removed en bloc, placed in embedding medium (Triangle Biomedical Sciences, Durham, NC), quickly frozen on dry ice, and stored at −70°C until they were processed for ISHH, which was performed as previously described by Gauda et al. (12). Tissue blocks were cut in 12-μm sections via cryostat, thaw mounted onto gelatin-chrome, alum-subbed slides, and fixed in 4% paraformaldehyde in 0.9% normal saline, acetylated in fresh acetic anhydride-triethanolamine, dehydrated in an ascending series of alcohols, delipidated in chloroform, and rehydrated in a descending series of alcohols. The full-length cDNA corresponding to the rat CB1R was cloned into the *Eco*RI site of Bluescript SK(+) to generate radioactive antisense ribonucleotide probes via in vitro transcription (clones kindly provided by Dr. Mary E. Abood, Forbes Norris ALA/MDA Research Center, California Pacific Medical Center, San Francisco, CA) (27).

Ribonucleotide probes were labeled with [^{35}S]UTP via in vitro transcription. Before hybridization, the sections were pretreated with proteinase K (2.5 μg/ml; Fisher Biotech, Fairlawn, NJ) for 10 min. Labeled probes of 1.2–1.5 × 10^6 disintegrations/min were added to 100 μl of hybridization buffer [50% formamide, 600 mM NaCl, 20 mM Tris·HCl (pH 7.5), 1 mM EDTA, 10% dextran sulfate, 1× Denhardt's solution, 100 μg/ml salmon sperm DNA, 250 μg/ml yeast total RNA (type XI, from bakers' yeast), 250 μg/ml yeast tRNA, and 100 mM dithiothreitol], which was applied to slides containing 8–10 sections per slide, and then coverslips were applied. Hybridization was performed at 55°C overnight. Coverslips were removed by four sequential 30-s washes in 1× SSC (0.15 M sodium chloride-0.015 M sodium citrate, pH 7.2) at room temperature. After treatment with RNase A (20 mg/ml; Sigma-Aldrich, St. Louis, MO) for 15 min at room temperature, slides were washed three times for 20 min in 0.2× SSC at 60°C, rinsed in deionized water, and air dried. Slides were then dipped in Kodak photographic emulsion (Eastman Kodak, Rochester, NY) diluted 1:1 with (0.6 M) ammonium acetate (Sigma-Aldrich), dried, and exposed in the dark at −20°C for 8–10 wk. After exposure, the slides were thawed at room temperature, developed with Dektol (diluted 1:1 with deionized H_2O; Eastman Kodak), fixed in Kodak Fixer, counterstained with thionin, dehydrated in an ascending series of alcohols, and cleared with xylenes, and then coverslips were applied with Permount.

For visualization of silver grains and ganglion cells in the same field, a combination of dark-field and phase-contrast light microscopy was used. Qualitative and semiquantitative analysis of CB1R mRNA expression was performed. Qualitative analysis was performed by showing the pattern of CB1R mRNA expression (silver grains) in the different tissues at the three postnatal ages. To determine the level of CB1R gene expression in the NG-PG-JG complex, semiquantitative analysis was performed by counting the silver grains generated by ^{35}S in the emulsion. Silver grains were analyzed using a Nikon microscope and Macintosh Image Analysis Program (National Institutes of Health Image, W. Rasband). Dark-field images were captured and digitized at ×400 and semiquantified by counting silver grains representing CB1R mRNA expression in the NG-PG-JG complex from animals at *DOL 5*, *7*, and *14*. Using a 60-μm-diameter circle, which is the approximate size of a ganglion cell, the number of silver grains was counted for 10 ganglion cells per tissue section, with 9 tissue sections counted per animal. The mean number of silver grains per ganglion cell per animal was determined, and comparisons were made between means obtained for each animal at *DOL 5*, *7*, and *14*.

Because the level of CB1R mRNA expression in the SCG was markedly lower than that of the NG-PG-JG complex, when the number of silver grains was counted in 30 randomly selected fields by the 60-μm-diameter circle method, there was no significant ($P > 0.05$) difference in the mean number of silver grains per ganglion cell per animal. However, qualitative analysis clearly demonstrated that postnatal development did affect the pattern of CB1R mRNA expression in the SCG. Thus, to determine the level of CB1R gene expression in the SCG, a different method of counting was employed. The number of silver grain clusters, defined as ≥15 silver grains per cluster, was counted for 5 randomly selected fields per section, with 4 tissue sections analyzed per animal, the mean number of silver grain clusters for each animal was obtained, and comparisons were made between animals at *DOL 5*, *7*, and *14*. To determine the differences in gene expression in the NG-PG-JG complex and the SCG, one-way ANOVA with post hoc analysis was used. Significance was accepted at $P < 0.05$. Comparisons were made only between data obtained from slides that were processed for ISHH simultaneously.

Western Blot Analysis

Protein homogenates of SCG, hippocampus, and cerebellum from animals at *DOL 12* and *33* were used to determine the molecular mass of the CB1R protein detected with the antibody used for IHC by methods similar to those described previously (33). The SCG, hippocampus, and cerebellum were dissected, frozen in isopentane, and then later homogenized with a Brinkman Polytron in ice-cold buffer consisting of 20 mM Tris·HCl, pH 7.4, containing 10% (wt/vol) sucrose, 20 μg/ml aprotinin (Trayslol), 20 μg/ml leupeptin, 20 μg/ml antipain, 20 μg/ml pepstatin A, 20 μg/ml chymostatin, 0.1 mM PMSF, 10 mM benzamidine, 1 mM EDTA, and 5 mM EGTA. The pellet was resuspended in homogenization buffer supplemented with 20% (wt/vol) glycerol, and protein concentrations were determined by Bradford assay. Homogenates of SCG, hippocampus, and cerebellum were fractionated by 10% SDS-PAGE (Sigma-Aldrich) and transferred to nitrocellulose membranes (Protran, Schleicher and Schuell BioScience, Keene, NH) by electroblotting (65–70 V for 2 h at room temperature). The reliability of sample loading and protein transfer was evaluated by staining nitrocellulose membranes with 5% Ponceau S red (Sigma-Aldrich) before immunoblotting and by quantification of Coomassie-stained (Bio-Rad Laboratories, Hercules, CA) gels by optical densitometry. Blots were blocked at room temperature with 2.5% nonfat dry milk containing 0.1% Tween 20 in 50 mM Tris-buffered saline (TBS; 50 mM Tris·HCl, pH 7.2, and 150 mM NaCl) for 1 h and then incubated overnight at 4°C with CB1R primary antibody (1:2,000; Sigma-Aldrich). After incubation with CB1R antibody, blots were washed and incubated with horseradish peroxidase-conjugated goat anti-rabbit IgG (1:500; Amersham Biosciences, Piscataway, NJ) for 1 h and developed with enhanced chemiluminescence (Amersham Biosciences) as recommended by the manufacturer.

IHC

Single immunolabeling and light microscopy. Similar to tissue preparation for ISHH, frozen tissue blocks of the carotid body, SCG, and NG-PG-JG complex were cut in 12-μm sections by cryostat. Slide-mounted sections were thaw mounted onto gelatin-chrome, alum-subbed slides fixed in 4% paraformaldehyde in 0.9% normal saline for 10 min, washed three times for 5 min with 1× TBS, pH 7, permeabilized in 100% ice-cold acetone for 10 min, and then washed three times with TBS. Tissue endoperoxidases were quenched in 3% hydrogen peroxide for 10 min. The slides were then washed three times with TBS, and nonspecific binding was blocked by incubating the slides in 10% BSA containing 0.1% Triton X-100 (Sigma-Aldrich) for 60 min at room temperature. The slides were incubated in CB1R antibody (1:2,000; Sigma-Aldrich) in 1× TBS containing 0.3% Triton X-100 and 3% BSA overnight at room temperature. The slides were then washed with 1× TBS and incubated with biotinylated donkey anti-rabbit antibody (1:200; Santa Cruz Biotechnology, Santa Cruz, CA) at room temperature for 2 h followed by streptavidin-horseradish peroxidase (BD Biosciences Pharmingen, San Diego, CA), and a visible reaction product was produced by treatment of the slides with 0.05% 3,3′-diaminobenzidine (DAB)-0.4% ammonium chloride-20% glucose (Sigma-Aldrich) and 51.45 U/μl glucose oxidase (1,029 U/ml; Fluka BioChemiKa, Buchs, Switzerland). Coverslips were

applied to the slides with Aqueous Mount (ScyTek Laboratories, Logan, UT).

Double-labeling immunofluorescence and confocal microscopy. A subgroup of animals was used to determine the number of tyrosine hydroxylase (TH)-immunoreactive cells in the NG-PG-JG complex that were coexpressed with CB1R-immunoreactive cells. Slides were processed as outlined above for single-labeled IHC for light microscopy with the following modifications for double-labeled immunofluorescence and confocal microscopy. All primary and secondary antibodies were diluted in 1× TBS containing 0.3% Triton X-100 and 3% BSA. The slides were incubated in primary CB1R rat antibody raised in rabbit (1:4,000; Sigma-Aldrich) overnight at room temperature, washed three times for 5 min with 1× TBS, and then incubated with Alexa Fluor 488 goat anti-rabbit secondary antibody (1 μg/ml; Molecular Probes, Eugene, OR) for 2 h at room temperature. Then the slides were washed with 1× TBS and incubated with mouse anti-TH monoclonal antibody (1:1,000; Chemicon International, Temecula, CA) in 1× TBS overnight at 4°C. The slides were washed three times with 1× TBS and incubated with tetramethylrhodamine isothiocyanate (rhodamine)-conjugated secondary antibody (1:400; Santa Cruz Biotechnology). Finally, slides were washed with 1× TBS, and coverslips were applied with ProLong antifade reagent (Molecular Probes).

Fluorescent images of the NG-PG-JG complex of three animals at *DOL 17* were captured at ×40 with a charge-coupled device camera (Photometrics CoolSnap FX) attached to a fluorescent microscope (Nikon Eclipse E-400) and stored in an image analysis program (IPLab, version 3.5). The fluorescent cells were detected using filters for rhodamine (absorption at 555 nm and emission at 580 nm) and for FITC (absorption at 494 nm and emission at 519 nm). Sequential capturing of both fluorescent images with each filter set was performed for each tissue section to determine coexpression of TH and CB1R immunoreactivity. Background fluorescence was subtracted for rhodamine and FITC tissue sections by comparison with sections that were processed without primary antibody. The percentage of TH-immunoreactive cells that coexpressed CB1R immunoreactivity was determined by counting all TH-immunoreactive cells and then counting the cells that also were positive for CB1R immunoreactivity in three to five sections per ganglion per animal. Only those TH-immunoreactive cells with easily discernable nuclei were counted.

Tissue sections were also examined by UltraView Confocal Imaging System (Perkin-Elmer Life and Analytical Sciences, Boston, MA) utilizing the Nipkow spinning disk, which was mounted onto a Zeiss Axiovert 200M inverted microscope equipped with a ×40 plan-fluor (1.3 numerical aperture) or a ×60 or ×100 plan (1.4 numerical aperture)-apochromat objective lens with corresponding 1-, 0.8-, and 0.45-μm optical *z*-slice 12-bit images (Hamamatsu Orca-ER CCD). Images were merged and analyzed with UltraView acquisition (Spatial Module) software and red-green-blue and colocalization analysis. Controls, processed in the absence of primary antibody, were used for background subtraction.

Immunoelectron Microscopy

Animals were anesthetized with pentobarbital sodium and perfused transcardially with ice-cold 1× PBS, pH 7.4, followed by 4% paraformaldehyde-0.1% glutaraldehyde diluted in 1× PBS, pH 7.4. The SCG and NG-PG-JG complex were dissected, and the brain was removed from animals at *DOL 25* and *35*. All tissues were postfixed for 2 h at 4°C, placed in 1× PBS, and refrigerated overnight. Free-floating sections of the SCG and NG-PG-JG complex were obtained by embedding the tissue en bloc in 3% sterile agar (Sigma-Aldrich) and cutting the agar blocks into 40-μm sections with a low-angle vibrating Vibratome (speed setting 2, amplitude 8.5, blade angle 30°; Ted Pella, Redding, CA) at 1°C. Free-floating tissue sections were washed in 1× TBS and then processed for detection of CB1R immunoreactivity, as outlined above for slides, with one exception: all tissue sections were incubated with CB1R antibody (1:500) diluted in 1× TBS containing 0.3% Triton X-100 and 3% BSA overnight. CB1R immunoreactivity was visualized using 0.05% DAB-0.4% ammonium chloride-20% glucose (Sigma-Aldrich) and 51.45 U/μl glucose oxidase (1,029 U/ml; Fluka BioChemiKa) for 10 min, rinsed in 1× PBS, and then processed for electron microscopy. Tissue sections were processed in the presence or absence of CB1R primary antibody simultaneously.

After immunostaining, tissue sections were flattened in petri dishes, and excess PBS was aspirated. Fixed 40-μm sections were washed in 0.1 M sodium cacodylate containing 3 mM $CaCl_2$, pH 7.4, at 4°C. Sections were osmicated in 2% osmium tetroxide containing 0.1 M sodium cacodylate and 3 mM $CaCl_2$ for 1 h at 4°C in the dark and then washed with deionized H_2O. Next, sections were dehydrated in an ascending series of alcohols, washed twice in propylene oxide, and infiltrated overnight in a 1:1 dilution of propylene oxide-Eponate 12 (EPON 812, Polysciences, Warrington, PA) containing the curing catalyst dimethylaminomethyl phenol (1.5%). On the next day, sections were embedded in Eponate 12 containing 1.5% dimethylaminomethyl phenol for 6 h. Sections were flat embedded between two sheets of Aclar fluoropolymer film (Ted Pella), weighted onto a hard flat surface, and heated at 60°C for 2 days. Sections were window-cut out with a razor blade and reembedded in an inverted BEEM capsule (Ted Pella) and cured. Blocks were trimmed on a Leica/Reichert Ultracut E ultramicrotome, faced with glass knives, and sectioned (200 nm) with a low-angle diamond knife (Diatome US). Ultrathin tissue sections were picked up with 2 × 1-mm Fomvar-coated slot grids (Ted Pella) and photographed on a Phillips CM 120 transmission electron microscope operating at 80 kV. Negatives were converted to TIFF images with an Epson Perfection 2450 photo scanner operating at 400 dpi.

RESULTS

ISHH

Constitutive CB1R gene expression during postnatal development. Constitutive expression of CB1R mRNA was detected in the NG-PG-JG complex, SCG, and carotid body. However, the level of CB1R mRNA expression differed among the three tissues. Specifically, CB1R mRNA was intensely expressed in many ganglion cells in the NG-PG-JG complex (Fig. 1*A*), less intensely expressed in a few to a moderate number of ganglion cells in the SCG (Fig. 1*B*), and barely expressed above background in the carotid body (Fig. 1, *C* and *D*). This relative pattern of constitutive expression of CB1R mRNA among the three different tissues was consistent throughout each of the three age groups studied. However, the level of mRNA expression within the three tissues was significantly affected by postnatal development, which was best demonstrated in the NG-PG-JG complex (Fig. 2). During postnatal development, CB1R mRNA levels significantly increased in the NG-PG-JG complex from 12.6 ± 2.06 to 23.9 ± 1.6 silver grains/ganglion cell ($P = 0.001$, 1-way ANOVA) from *DOL 5* to *DOL 7*, with no further change at *DOL 14* (Fig. 2).

CB1R mRNA expression in the SCG also changed with postnatal development. This change in CB1R mRNA expression in the SCG was not reflected in the average number of silver grains per ganglion cell when the average number of silver grains per ganglion cell was calculated for 30 ganglion cells in the SCG and the mean was obtained for each of the 3 age groups. However, postnatal development did affect the pattern of CB1R mRNA expression in the SCG, as shown in representative photomicrographs from three animals (Fig. 3). A

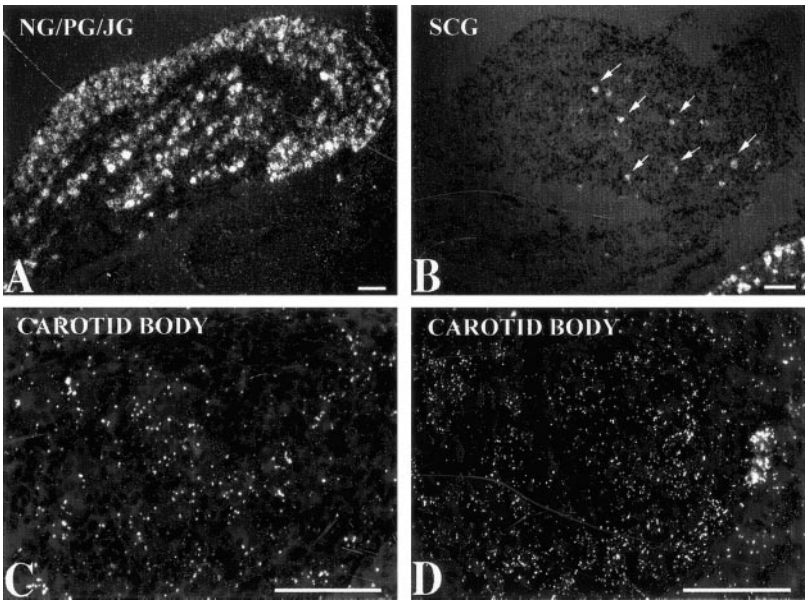

Fig. 1. Photomicrographs of dark-field images showing expression pattern for cannabinoid receptor type 1 (CB1R) mRNA in the nodose-petrosal-jugular ganglia (NG-PG-JG) complex (*A*), superior cervical ganglion (SCG, *B*), and carotid body (*C* and *D*). CB1R mRNA is expressed in many cells in the NG-PG-JG complex and a few cells in the SCG (*B*) and has a diffuse pattern of low-level expression in the carotid body, as seen in 1 representative animal at *day of life* (*DOL*) *5* (*C*), and a moderate level of expression in a representative animal at *DOL 14* (*D*). Silver grains are depicted as clusters of white dots (arrows). Scale bars, 50 μm.

low-level diffuse expression of CB1R mRNA was seen in many ganglion cells in the SCG at *DOL 5* (Fig. 3*A*). During the first 2 wk of postnatal development, the number of silver grains per ganglion cell significantly increased, resulting in CB1R mRNA expression appearing as clusters of silver grains in the ganglion cells of animals at *DOL 14* (Fig. 3*C*). An intermediate pattern was observed in sections of the SCG from animals at *DOL 7* (Fig. 3*B*). The mean number of silver grain clusters per SCG increased with postnatal development: 4.83 ± 0.65 at *DOL 5*, 7.0 ± 0.84 at *DOL 7*, and 17.4 ± 1.96 at *DOL 14* ($P = 0.001$, 1-way ANOVA; Fig. 3). The low-level expression of CB1R mRNA in the carotid body of animals in each age group did not allow for reliable semiquantitative analysis.

The pattern of CB1R mRNA expression in brain sections (hippocampus and striatum), which were simultaneously processed, hybridized, exposed, and developed with slides of the NG-PG-JG complex, SCG, and carotid body, exhibited the characteristic pattern of expression that has been previously described (45) (data not shown).

Western Blot Analysis

CB1R protein size in brain and autonomic ganglia. Western blot analysis of homogenates of the hippocampus and cerebellum (at *DOL 33*; controls) and the SCG (at *DOL 12* and *33*) was performed with affinity-purified CB1R antibodies to determine whether the antibody was recognizing the same protein in the central nervous system (CNS) and PNS. Three immunoreactive protein bands were detected in homogenates of the hippocampus and cerebellum with affinity-purified CB1R antibodies, whereas only two immunoreactive bands were evident in homogenates of the SCG at *DOL 12* and *33* (Fig. 4). Bands of ~69 and ~49 kDa were found in the hippocampus, cerebellum, and SCG. The ~33-kDa band was detected only in

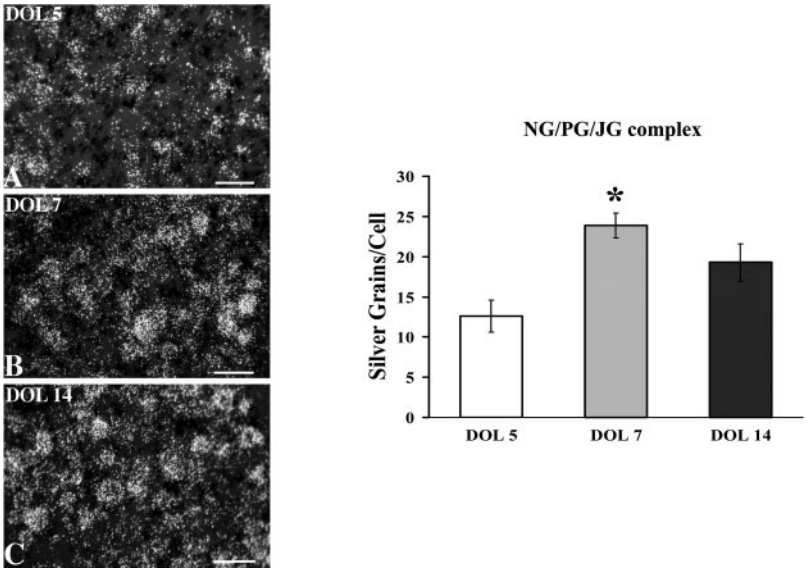

Fig. 2. Ontogeny of CB1R mRNA expression in the NG-PG-JG complex. Photomicrographs of dark-field images of the NG-PG-JG complex show expression of CB1R mRNA in representative animals at *DOL 5* (*A*), *7* (*B*), and *14* (*C*). CB1R mRNA expression is depicted as clusters of silver grains (white dots). Bar graph depicts significant increase in CB1R mRNA expression from *DOL 5* to *DOL 7*, with no further increase by *DOL 14*. Values are means ± SE; $n = 5$. *$P < 0.001$ vs. *DOL 5*.

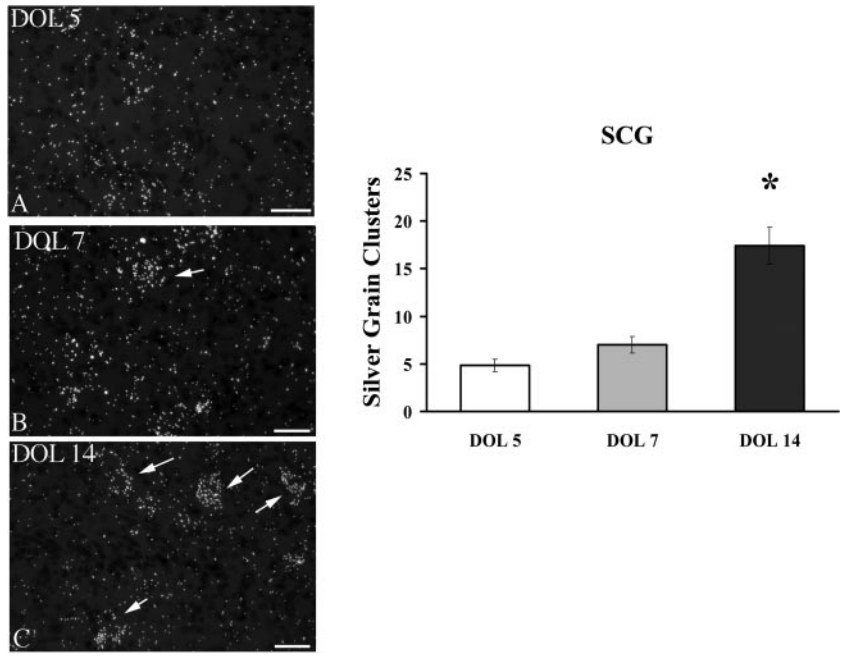

Fig. 3. Ontogeny of CB1R mRNA expression in the SCG. Photomicrographs of dark-field images of the SCG show change in pattern of expression of CB1R mRNA in 3 representative animals at *DOL 5* (*A*), *7* (*B*), and *14* (*C*). CB1R mRNA expression is depicted as clusters of silver grains (white dots). Bar graph depicts significant increase in clusters (arrows) of CB1R mRNA expression in the SCG from *DOL 5* to *DOL 14*. Bar graph shows CB1R levels in the NG-PG-JG complex of animals at *DOL 5*, *7*, and *14*. Values are means ± SE; $n = 5$. *$P < 0.001$ vs. *DOL 5* (1-way ANOVA with post hoc analysis).

homogenates of the hippocampus and cerebellum, but not in the SCG.

Light and Confocal Microscopy

Single-labeled CB1R and TH immunoreactivity. CB1R immunoreactivity was present in numerous ganglion cells in the SCG and NG-PG-JG complex, as seen in the photomicrograph of the SCG (Fig. 5, *A–D*) and NG-PG-JG complex (Fig. 5, *E* and *F*) from an animal at *DOL 14*. Interestingly, CB1R immunoreactivity, with DAB as the chromagen, was intensely localized to the nucleus of these ganglion cells. Similarly, visualization of fluorescent CB1R immunoreactivity by confocal microscopy localized CB1R immunoreactivity to the nucleus. NG-PG-JG complex tissue sections double labeled with Alexa Fluor 488 for detection of CB1R immunoreactivity and with tetramethylrhodamine isothiocyanate for detection of TH immunoreactivity also showed cytoplasmic localization of the TH immunoreactivity (Fig. 6*A*, red), as expected, and nuclear localization of CB1R immunoreactivity (Fig. 6*B*, green). Although 64% of the ganglion cells in the NG-PG-JG complex that were positive for TH immunoreactivity were also positive for CB1R immunoreactivity, colocalization of the these proteins within the same subcellular compartment was not evident, because essentially no ganglion cells showed yellow staining indicative of the presence of both fluorochromes. Furthermore, in the carotid body, CB1R immunoreactivity was not colocalized with TH immunoreactivity, suggesting that type I (glomus) cells of the carotid body do not express CB1R. Alternatively, the level of expression was below the level of detection.

As previously described by others, there was clear localization of the CB1R immunoreactivity in the cytoplasm of cortical (Fig. 7, *A* and *B*) and hippocampal (Fig. 7, *C* and *D*) neurons (35, 45). No nuclear expression of CB1R was found in neurons of the CNS. Cortical and hippocampal sections were processed together with SCG and NG-PG-JG complex sections. The same pattern of immunoreactivity was seen whether IHC was performed on slides or on free-floating sections, and the pattern of expression was identical at all ages studied (data not shown).

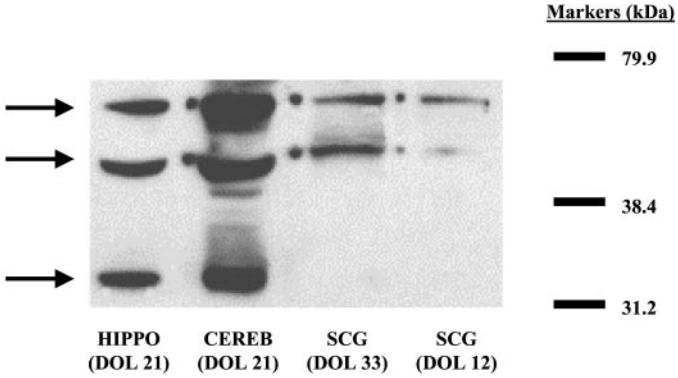

Fig. 4. Western blot analysis of CB1R immunoreactivity in rat brain and SCG. Membrane proteins were obtained from homogenates of hippocampus (Hippo) and cerebellum (Cereb) from 1 animal at *DOL 33* and homogenates of the SCG from animals at *DOL 33* and *12*. In the lane containing crude protein extract from the hippocampus and cerebellum, 3 protein bands of ~69, ~49, and ~33 kDa (arrows) were present. Protein bands at ~49 and ~33 kDa were also easily seen in the lane containing crude proteins from the SCG in animals in both age groups.

Electron Microscopy

Nuclear localization of CB1R immunoreactivity in the SCG. Immunoelectron microscopy confirmed the subcellular localization of CB1R immunoreactivity that was observed by light and confocal microscopy. Free-floating tissue sections of the SCG and NG-PG-JG complex embedded in agar and hippocampal tissue sections were processed together for immunoelectron microscopy, with DAB as the chromagen. As shown in the representative photomicrograph from an animal at *DOL 25*, the reaction product was localized to the nucleus of a ganglion cell of the SCG (Fig. 8*A*) and to the nucleus and cytoplasm of another ganglion cell from the same tissue block

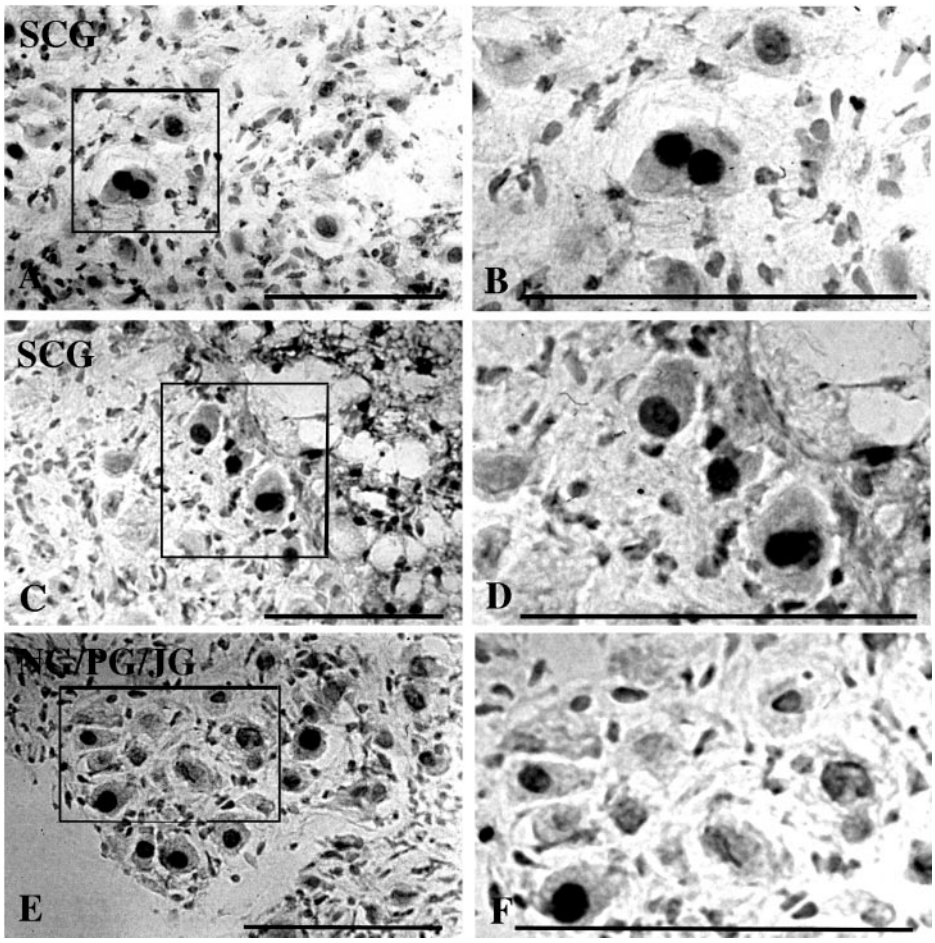

Fig. 5. Photomicrographs of low-power (*A*, *C*, and *E*; squares) and high-power (*B*, *D*, and *F*) bright-field images of immunohistochemistry, with 3,3′-diaminobenzidine (DAB) as the chromagen, show CB1R immunoreactivity localized to the nucleus of ganglion cells in the SCG (*A–D*) and NG-PG-JG complex (*E* and *F*) in images from 1 representative animal at *DOL 17*. Scale bars, 50 μm.

(Fig. 8*B*). No reaction product was seen in tissue sections that were processed without the primary antibody (Fig. 8*C*). In agreement with our light and confocal microscopy findings, immunoelectron microscopy confirmed that CB1R expression was confined to the cytoplasm of hippocampal neurons (Fig. 9).

DISCUSSION

The major findings from this study are as follows: *1*) CB1R mRNA is expressed within the peripheral arterial chemoreceptors, with the greatest expression in the NG-PG-JG complex, moderate expression in the SCG, and minimal expression in the carotid body, and the level of expression in these tissues increases with postnatal age. *2*) The CB1R is localized to the nuclei of ganglion cells in sensory and autonomic ganglia, which contrasts sharply with the cytoplasmic localization of this receptor in cortical and hippocampal neurons. *3*) TH and CB1R immunoreactivity are coexpressed in a subset of petrosal ganglion neurons. Because nerve fibers from preganglionic parasympathetic and postganglionic sympathetic nerve fibers innervate blood vessels within the carotid body and petrosal ganglion cells contain the cell bodies of chemoafferents, localization of CB1R mRNA and protein to these ganglion cells suggests that exogenous and endogenous cannabinoid exposure

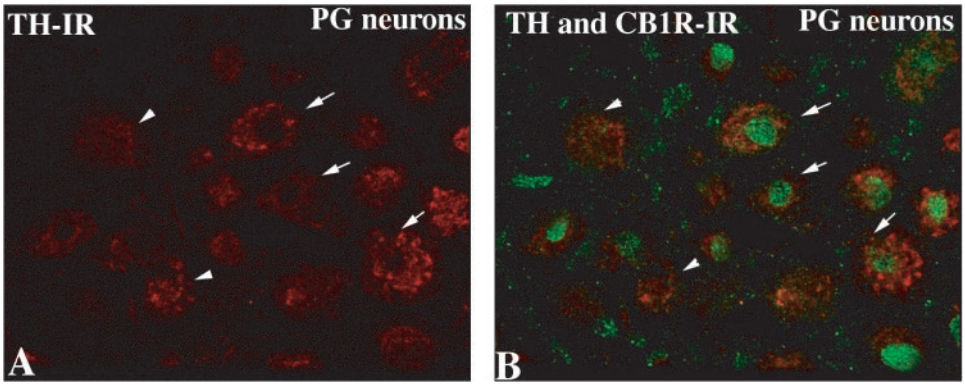

Fig. 6. Photomicrograph of tissues double labeled to detect CB1R and tyrosine hydroxylase (TH) immunoreactivity (IR) in ganglion cells of the NG-PG-JG complex using confocal microscopy at high magnification (×40). TH immunoreactivity (red, *A*) was localized to the cytoplasm in the same cells that contained nuclear localization of CB1R immunoreactivity (green, *B;* arrows). Some cells contained only TH immunoreactivity (*A* and *B;* arrowheads). Colocalization of immunoreactivity within the same subcellular compartment was not evident, because essentially no ganglion cells showed yellow color, indicative of colocalization.

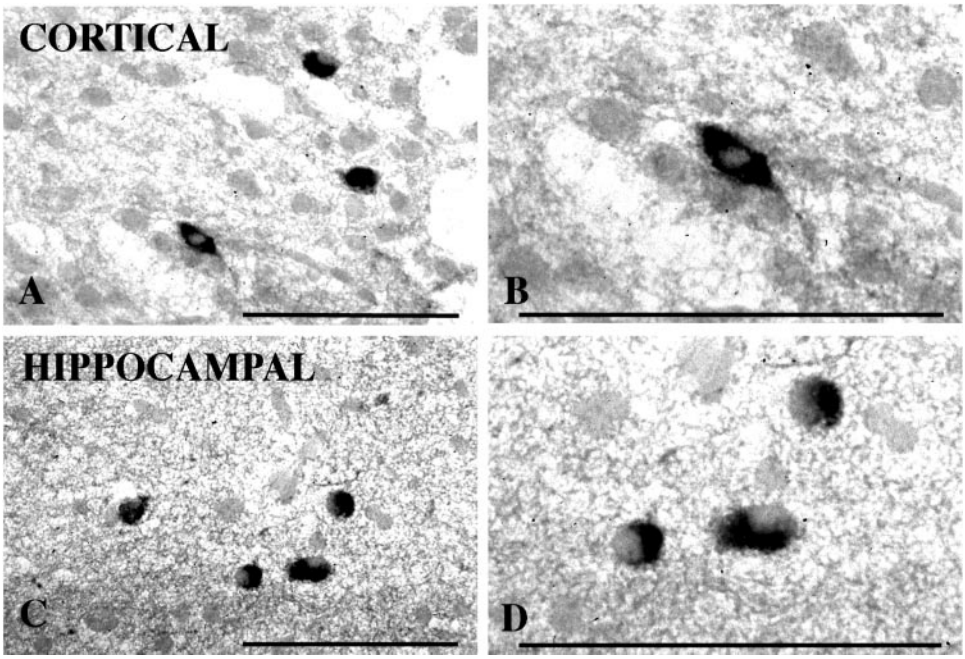

Fig. 7. Photomicrographs of low-power (*A* and *B*) and high-power (*B* and *D*) bright-field images of immunohistochemistry, with DAB as the chromagen, show CB1R immunoreactivity in the cytoplasm of cortical (*A* and *B*) and hippocampal (*C* and *D*) neurons in 1 representative animal at *DOL 17*. Scale bars, 25 μm.

could affect chemoreceptor function during early postnatal development.

Cannabinoids, a family of cell membrane-derived signaling molecules released from nerve, blood, and endothelial cells, have diverse biological effects, including actions on the immune and cardiovascular systems, CNS, and PNS (37). CB1Rs are GPCRs and, along with their endogenous ligands, exist as part of an endogenous cannabinoid system in the CNS as well as the PNS. This endocannabinoid system has been shown to participate in the development of the CNS and PNS (2). Perinatal exposure to cannabinoids alters the developmental profile of several brain dopaminergic systems and causes important changes in the function of these systems on a neurochemical and a behavioral level in adult rats (40).

Endogenous and exogenous cannabinoids also modulate the activity of the sympathetic nervous system. CB1R activation induces sympathoinhibition and enhances cardiac vagal tone, leading to hypotension and bradycardia (32), through a peripheral mechanism. Specifically, cannabinoids cause presynaptic inhibition of the release of norepinephrine from terminals of postganglionic sympathetic neurons (17), whereas local injection of CB1R agonists into the nucleus tractus solitarius or rostral ventrolateral medulla does not affect heart rate or blood pressure or minimally reduces blood pressure, respectively (32). Similar to the results reported by Ishac et al. (17), we suggest that CB1R mRNA and protein are present in cell bodies of postganglionic neurons in the SCG. Nerve fibers from these postganglionic cells innervate the carotid body and its blood vessels via the ganglioglomerular and carotid sinus nerves (49). Thus endogenous and exogenous cannabinoids may affect local blood flow within the carotid body, thereby changing the level of oxygen tension within the carotid body and, thus, modifying activity from the carotid body.

Exposure to exogenous cannabinoids (THC) also affects respiration in humans (18, 24, 25); however, depending on the route of administration and the frequency of use, the respiratory response in humans varies from depression to no effect. Consistent respiratory depression has been reported in spontaneously breathing (47) and anesthetized (32, 41) animals. Although respiratory depression in response to THC can be centrally mediated (29, 44), we now demonstrate that CB1R mRNA is found in the carotid body and in a large population of cell bodies of neurons in the glossopharyngeal and vagal sensory (jugular, petrosal, and nodose) ganglia, the major source of visceral afferent innervation, which contain the perikarya of vagal afferent neurons that function as cardiopulmonary receptors and aortic baroreceptors. Thus it is possible, as suggested by Schmid et al. (41), that the respiratory depression associated with exogenous cannabinoid exposure may involve peripheral arterial chemoreceptors, suggesting that endocannabinoids may have important influences on several aspects of respiratory control. In addition, SCG and vagal neurons may modulate other autonomic functions. Our findings of *1*) low levels of CB1R mRNA expression in the carotid body, *2*) CB1R mRNA and protein expression in ganglion cells in the NG-PG-JG complex, and *3*) coexpression of CB1R and TH immunoreactivity in the perikarya of putative chemoafferents support this speculation.

The prominent nuclear localization of CB1R immunoreactivity within sensory and autonomic ganglion cells was an unexpected finding and differed from the cytoplasmic localization of CB1R immunoreactivity in cortical and hippocampal neurons. CB1R is a member of the superfamily of transmembrane GPCRs. Similar to other pertussis toxin-sensitive GPCRs, ligand binding to CB1Rs inhibits adenylyl cyclase, activates inwardly rectifying K^+ channels, and inhibits N-, P/Q-, L-, and T-type Ca^{2+} channels (5, 35). Ligand binding to membrane-bound GPCRs also triggers a cascade of intracellular events, leading to activation of transcription factors in the nucleus and translocation of other signaling molecules from the cytoplasm to the nucleus. After agonist stimulation, translocation of the M_2-muscarinic acetylcholine receptor and the D_1-dopamine receptor from axons to the soma or perinuclear

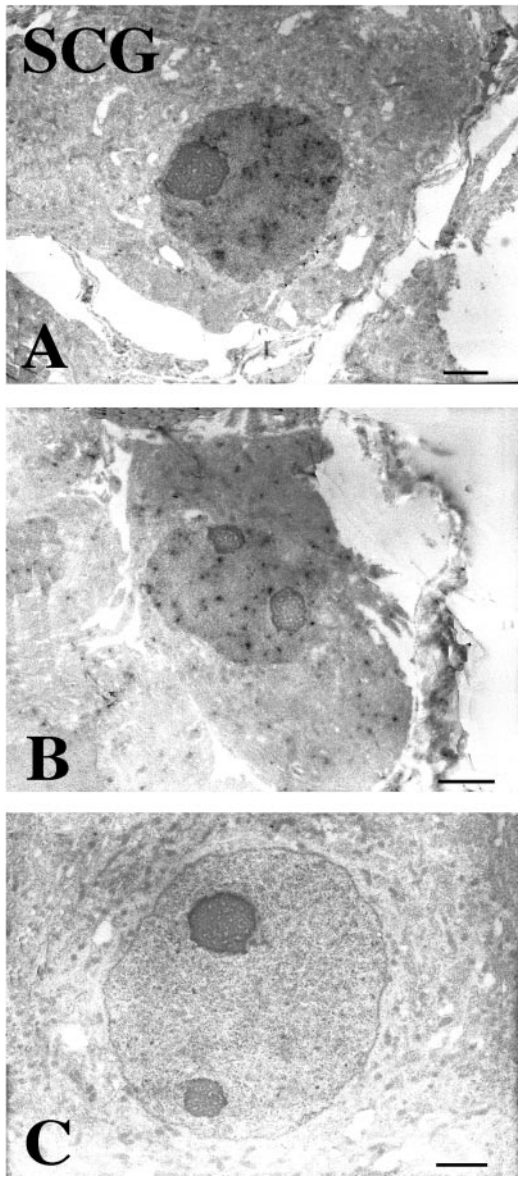

Fig. 8. Electron photomicrographs showing subcellular localization of CB1R immunoreactivity in the SCG. Reaction product (DAB) representing CB1R immunoreactivity was localized to the nucleus (*A*) in most of the ganglion cells examined. In a few ganglion cells, reaction product was seen in the nucleus and cytoplasm (*B*). No reaction product was seen in electron micrograph sections processed in the absence of primary antibody (*C*). Scale bars, 2 nm.

endosomes has been described in striatal interneurons and in mesostriatal dopaminergic neurons (1, 8).

Intracellular translocation has also been described for the CB1R. Using the same primary antibody that we used in our studies, Coutts et al. (6) showed that CB1Rs translocate from axons to the soma of cultured hippocampal neurons from rats. Similarly, CB1Rs have been shown to translocate toward the soma in F-11 cells, which constitutively expresses CB1R, and in Chinese hamster ovary cells, which were transfected with CB1R cDNA (39).

Although translocation of neuronal GPCRs to the soma and perinuclear endosomes in response to agonist activation appears to be most commonly described, specific nuclear localization or translocation of GPCRs to the nucleus has been described for only one GPCR, lysophosphatidate receptor (LPA_1). Moughal et al. (30) reported that LPA_1, a GPCR that interacts with the tyrosine kinase receptor (Trk A) to regulate p42/p44 MAPK in PC12 cells, is translocated to the nucleus on agonist activation. We have now confirmed localization of the CB1R to the nucleus of ganglion cells in sensory and autonomic sympathetic ganglia with confocal and immunoelectron microscopy; the functional significance of this novel finding remains to be determined.

In addition to the nuclear localization of CB1R in the tissue sections prepared for immunoelectron microscopy, CB1R was also found in the cytoplasm and the plasma membrane in a few ganglion cells in the petrosal ganglion. This was not apparent on sections assessed with light microscopy. What remains to be determined is why CB1R is preferentially found in the cytoplasm of ganglion cells within the CNS and preferentially localized to the nucleus of ganglion cells in the PNS and how agonist stimulation may alter the subcellular expression of CB1Rs in the PNS.

Multiple control experiments were performed to determine whether the different patterns of immunostaining found in the CNS vs. autonomic and sensory ganglion cells of the peripheral arterial chemoreceptors was an artifact. IHC was performed on the following tissue preparations: *1*) fresh-frozen, *2*) paraformaldehyde-fixed, *3*) paraformaldehyde- and glutaraldehyde-fixed, and *4*) free-floating paraformaldehyde- and glutaraldehyde-fixed. The same pattern of immunoreactivity was seen whether IHC was performed on slides or on free-floating tissue or on fresh-frozen or fixed tissue sections, and the pattern of expression was identical at all ages studied. Additionally, Western blot analysis was performed on crude protein homogenates of the hippocampus, cerebellum, and SCG to

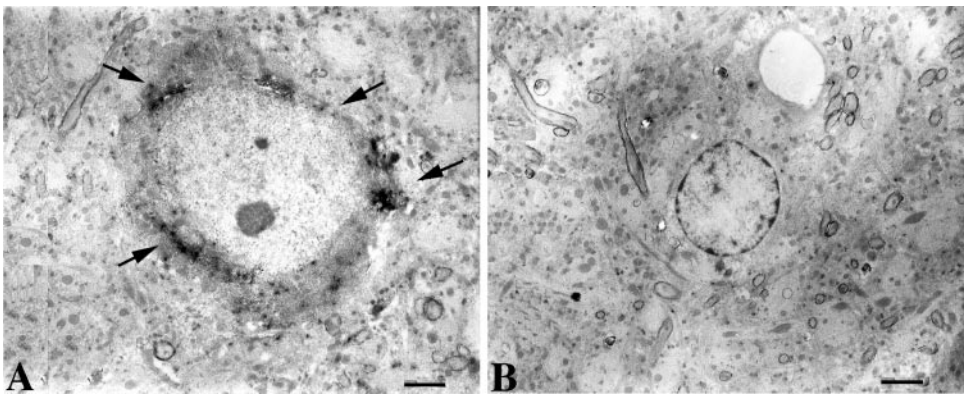

Fig. 9. Electron photomicrographs showing subcellular localization of CB1R immunoreactivity in hippocampal neurons of animals at *DOL 35*. Reaction product (DAB) representing CB1R immunoreactivity was localized to the cytoplasm of hippocampal neurons (*A*; arrows). No reaction product was seen in electron micrograph sections processed in the absence of primary antibody (*B*). Scale bars, 2 nm.

verify that the CB1R antibody recognized similar proteins in tissue from the CNS and peripheral ganglion cells. Western blot analysis of the hippocampus, cerebellum, and SCG with CB1R affinity-purified antibodies revealed ~69- and 49-kDa immunoreactive bands, which are consistent with the glycosylated and nonglycosylated forms of the CB1R, respectively, as detected in rat brain (43). The lower-molecular-mass (~33-kDa) band, detected only in homogenates of hippocampus and cerebellum, may have resulted from enzymatic degradation or may be a splice variant of the CB1R. We also used a CB1R antibody that has been well characterized and used extensively in IHC experiments to localize CB1R immunoreactivity in the brain. Furthermore, in each of our IHC experiments, we used *1*) brain tissue as a positive control, *2*) light, confocal, and electron microscopy to confirm our findings, and *3*) DAB and fluorescent chromogens. Thus we believe that, with the localization techniques available to us, we have substantiated our findings.

In addition to the known effects of cannabinoids on norepinephrine release, CB1Rs have other unique features that may result in altered neurotransmission of neurotransmitter systems that signal via pertussis toxin-sensitive G proteins. Specifically, the CB1R can sequester G proteins from a common intracellular pool and, thereby, prevent other GPCRs (specifically, $G_{i/o}$-coupled receptors) from signaling. This feature has been described by Vasquez and Lewis (46), who showed, in dissociated SCG neurons transfected with human CB1R cDNA, that signaling by the α_2-adrenergic receptor in response to norepinephrine was abolished by the active and inactive states of the human CB1R (46). CB1R stimulation can also inhibit new synapse formation (20). These properties of CB1Rs are likely relevant to neurotransmission within the carotid body, particularly during late fetal and early postnatal maturation, when the neuronal circuitry involved in chemotransduction is maturing.

In the CNS, CB1Rs colocalize with other neurotransmitters, specifically dopamine and serotonin (16), which modulate cardiorespiratory responses and the level of arousal from sleep. In the PNS, several GPCRs are involved in hypoxic chemotransmission in the carotid body (15). D_2-dopamine receptors are GPCRs that are coupled to $G_{i/o}$ and, therefore, negatively coupled to adenylyl cyclase. CB1Rs and D_2-dopamine receptors colocalize in neurons of the striatum (16), and ligand binding to CB1Rs inhibits D_2-dopamine receptor signaling (3). Dopamine and D_2-dopamine receptors are also present in ganglion cells of the SCG and petrosal ganglion (15). Potentially, CB1Rs may modify D_2-dopamine receptor signaling within these cells and, thus, alter hypoxic chemotransmission secondarily. During early development, the presence of CB1Rs within peripheral and central structures, which regulate cardiorespiratory control and arousal, could potentially lead to altered cardiorespiratory control as a result of chronic or acute exposure to exogenous cannabinoids.

In summary, we demonstrate that CB1Rs are found in peripheral arterial chemoreceptors, specifically, in the NG-PG-JG complex and, to a lesser extent, in the SCG and carotid body. CB1R mRNA expression significantly increases in the NG-PG-JG complex during the first 2 wk of postnatal development. Our data suggest that CB1Rs are uniquely positioned to modulate the function of peripheral arterial chemoreceptors by modifying signaling of other GPCRs involved in hypoxic chemotransmission or by participating in plasticity-induced changes in peripheral arterial chemoreceptors during development. Our findings may provide a possible biological explanation for the clinical observation that there is an increased risk of SIDS in infants exposed to marijuana during the perinatal period (21, 42).

ACKNOWLEDGMENTS

The authors thank Debra L. Flock for expertise in Western blot analysis, Michael J. Delannoy for assistance with immunoelectron microscopy and confocal imaging, and Nnamdi Ofoegbu for technical assistance.

GRANTS

This study was supported by National Institute on Drug Abuse Grant R01 DA-13940 (E. B. Gauda and G. L. McLemore).

REFERENCES

1. **Bernard V, Laribi O, Levey AI, and Bloch B.** Subcellular redistribution of m_2 muscarinic acetylcholine receptors in striatal interneurons in vivo after acute cholinergic stimulation. *J Neurosci* 18: 10207–10218, 1998.
2. **Buckley NE, Hansson S, Harta G, and Mezey E.** Expression of the CB1 and CB2 receptor messenger RNAs during embryonic development in the rat. *Neuroscience* 82: 1131–1149, 1998.
3. **Cadogan AK, Alexander SP, Boyd EA, and Kendall DA.** Influence of cannabinoids on electrically evoked dopamine release and cyclic AMP generation in the rat striatum. *J Neurochem* 69: 1131–1137, 1997.
4. **Carley DW, Paviovic S, Janelidze M, and Radulovacki M.** Functional role for cannabinoids in respiratory stability during sleep. *Sleep* 25: 391–398, 2002.
5. **Chemin J, Monteil A, Perez-Reyes E, Nargeot J, and Lory P.** Direct inhibition of T-type calcium channels by the endogenous cannabinoid anandamide. *EMBO J* 20: 7033–7040, 2001.
6. **Coutts AA, Anavi-Goffer S, Ross RA, MacEwan DJ, Mackie K, Pertwee RG, and Irving AJ.** Agonist-induced internalization and trafficking of cannabinoid CB1 receptors in hippocampal neurons. *J Neurosci* 21: 2425–2433, 2001.
7. **Day NL and Richardson GA.** Prenatal marijuana use: epidemiology, methodologic issues, and infant outcome. *Clin Perinatol* 18: 77–91, 1991.
8. **Dumartin B, Caille I, Gonon F, and Bloch B.** Internalization of D_1 dopamine receptor in striatal neurons in vivo as evidence of activation by dopamine agonists. *J Neurosci* 18: 1650–1661, 1998.
9. **Feng T.** Substance abuse in pregnancy. *Curr Opin Obstet Gynecol* 5: 16–23, 1993.
10. **Fewell JE, Taylor BJ, Kondo CS, Dascalu V, and Filyk SC.** Influence of carotid denervation on the arousal and cardiopulmonary responses to upper airway obstruction in lambs. *Pediatr Res* 28: 374–378, 1990.
11. **Franco P, Szliwowski H, Dramaix M, and Kahn A.** Decreased autonomic responses to obstructive sleep events in future victims of sudden infant death syndrome. *Pediatr Res* 46: 33–39, 1999.
12. **Gauda EB, Cooper R, Akins PK, and Wu G.** Prenatal nicotine affects catecholamine gene expression in newborn rat carotid body and petrosal ganglion. *J Appl Physiol* 91: 2157–2165, 2001.
13. **Gerard CM, Mollereau C, Vassart G, and Parmentier M.** Molecular cloning of a human cannabinoid receptor which is also expressed in testis. *Biochem J* 279: 129–134, 1991.
14. **Golding J.** Sudden infant death syndrome and parental smoking—a literature review. *Paediatr Perinat Epidemiol* 11: 67–77, 1997.
15. **González C, Dinger B, and Fidone S.** Functional significance of chemoreceptor cell neurotransmitters. In: *The Carotid Body Chemoreceptors*, edited by González C. Heidelberg: Springer-Verlag, 1997, p. 47–64.
16. **Hermann H, Marsicano G, and Lutz B.** Coexpression of the cannabinoid receptor type 1 with dopamine and serotonin receptors in distinct neuronal subpopulations of the adult mouse forebrain. *Neuroscience* 109: 451–460, 2002.
17. **Ishac EJ, Jiang L, Lake KD, Varga K, Abood ME, and Kunos G.** Inhibition of exocytotic noradrenaline release by presynaptic cannabinoid CB1 receptors on peripheral sympathetic nerves. *Br J Pharmacol* 118: 2023–2028, 1996.
18. **Johnstone RE, Lief PL, Kulp RA, and Smith TC.** Combination of Δ^9-tetrahydrocannabinol with oxymorphone or pentobarbital: effects on ventilatory control and cardiovascular dynamics. *Anesthesiology* 42: 674–684, 1975.

19. **Kato I, Franco P, Groswasser J, Scaillet S, Kelmanson I, Togari H, and Kahn A.** Incomplete arousal processes in infants who were victims of sudden death. *Am J Respir Crit Care Med* 168: 1298–1303, 2003.
20. **Kim D and Thayer SA.** Cannabinoids inhibit the formation of new synapses between hippocampal neurons in culture. *J Neurosci* 21: 1–5, 2001.
21. **Klonoff-Cohen H and Lam-Kruglick P.** Maternal and paternal recreational drug use and sudden infant death syndrome. *Arch Pediatr Adolesc Med* 155: 765–770, 2001.
22. **Legido A.** Intrauterine exposure to drugs [in Spanish]. *Rev Neurol* 25: 691–702, 1997.
23. **Ling L, Olson EB Jr, Vidruk EH, and Mitchell GS.** Phrenic responses to isocapnic hypoxia in adult rats following perinatal hyperoxia. *Respir Physiol* 109: 107–116, 1997.
24. **Malit LA, Johnstone RE, Bourke DI, Kulp RA, Klein V, and Smith TC.** Intravenous Δ^9-tetrahydrocannabinol: effects of ventilatory control and cardiovascular dynamics. *Anesthesiology* 42: 666–673, 1975.
25. **Mathew RJ, Wilson WH, Humphreys DF, Lowe JV, and Wiethe KE.** Regional cerebral blood flow after marijuana smoking. *J Cereb Blood Flow Metab* 12: 750–758, 1992.
26. **Matsuda LA, Lolait SJ, Brownstein MJ, Young AC, and Bonner TI.** Structure of a cannabinoid receptor and functional expression of the cloned cDNA. *Nature* 346: 561–564, 1990.
27. **McLaughlin CR and Abood ME.** Developmental expression of cannabinoid receptor mRNA. *Brain Res Dev Brain Res* 76: 75–78, 1993.
28. **Mitchell EA, Tuohy PG, Brunt JM, Thompson JM, Clements MS, Stewart AW, Ford RP, and Taylor BJ.** Risk factors for sudden infant death syndrome following the prevention campaign in New Zealand: a prospective study. *Pediatrics* 100: 835–840, 1997.
29. **Moss IR and Friedman E.** Δ^9-tetrahydrocannabinol: depression of ventilatory regulation; other respiratory and cardiovascular effects. *Life Sci* 19: 99–104, 1976.
30. **Moughal NA, Waters C, Sambi B, Pyne S, and Pyne NJ.** Nerve growth factor signaling involves interaction between the Trk A receptor and lysophosphatidate receptor 1 systems: nuclear translocation of the lysophosphatidate receptor 1 and Trk A receptors in pheochromocytoma 12 cells. *Cell Signal* 16: 127–136, 2004.
31. **Munro S, Thomas KL, and Abu-Shaar M.** Molecular characterization of a peripheral receptor for cannabinoids. *Nature* 365: 61–65, 1993.
32. **Niederhoffer N, Schmid K, and Szabo B.** The peripheral sympathetic nervous system is the major target of cannabinoids in eliciting cardiovascular depression. *Naunyn Schmiedebergs Arch Pharmacol* 367: 434–443, 2003.
33. **Northington FJ, Ferriero DM, Flock DL, and Martin LJ.** Delayed neurodegeneration in neonatal rat thalamus after hypoxia-ischemia in apoptosis. *J Neurosci* 21: 1931–1938, 2001.
34. **Pertwee R.** The evidence for the existence of cannabinoid receptors. *Gen Pharmacol* 24: 811–824, 1993.
35. **Pertwee RG.** Pharmacology of cannabinoid CB1 and CB2 receptors. *Pharmacol Ther* 74: 129–180, 1997.
36. **Prabhakar NR, Kou YR, and Kumar GK.** G proteins in carotid body chemoreception. *Biol Signals* 4: 271–276, 1995.
37. **Ralevic V.** Cannabinoid modulation of peripheral autonomic and sensory neurotransmission. *Eur J Pharmacol* 472: 1–21, 2003.
38. **Ralevic V, Kendall DA, Randall MD, and Smart D.** Cannabinoid modulation of sensory neurotransmission via cannabinoid and vanilloid receptors: roles in regulation of cardiovascular function. *Life Sci* 71: 2577–2594, 2002.
39. **Rinaldi-Carmona M, Le Duigou A, Oustric D, Barth F, Bouaboula M, Carayon P, Casellas P, and Le Fur G.** Modulation of CB1 cannabinoid receptor functions after a long-term exposure to agonist or inverse agonist in the Chinese hamster ovary cell expression system. *J Pharmacol Exp Ther* 287: 1038–1047, 1998.
40. **Rodriguez DF, Cebeira M, Fernandez-Ruiz JJ, Navarro M, and Ramos JA.** Effects of pre- and perinatal exposure to hashish extracts on the ontogeny of brain dopaminergic neurons. *Neuroscience* 43: 713–723, 1991.
41. **Schmid K, Niederhoffer N, and Szabo B.** Analysis of the respiratory effects of cannabinoids in rats. *Naunyn Schmiedebergs Arch Pharmacol* 368: 301–308, 2003.
42. **Scragg RK, Mitchell EA, Ford RP, Thompson JM, Taylor BJ, and Stewart AW.** Maternal cannabis use in the sudden death syndrome. *Acta Paediatr* 90: 57–60, 2001.
43. **Song C and Howlett AC.** Rat brain cannabinoid receptors are N-linked glycosylated proteins. *Life Sci* 56: 1983–1989, 1995.
44. **Szabo B, Siemes S, and Wallmichrath I.** Inhibition of GABAergic neurotransmission in the ventral tegmental area by cannabinoids. *Eur J Neurosci* 15: 2057–2061, 2002.
45. **Tsou K, Brown S, Sanudo-Pena MC, Mackie K, and Walker JM.** Immunohistochemical distribution of cannabinoid CB1 receptors in the rat central nervous system. *Neuroscience* 83: 393–411, 1998.
46. **Vasquez C and Lewis DL.** The CB1 cannabinoid receptor can sequester G-proteins, making them unavailable to couple to other receptors. *J Neurosci* 19: 9271–9280, 1999.
47. **Vivian JA, Kishioka S, Butelman ER, Broadbear J, Lee KO, and Woods JH.** Analgesic, respiratory and heart rate effects of cannabinoid and opioid agonists in rhesus monkeys: antagonist effects of SR 141716A. *J Pharmacol Exp Ther* 286: 697–703, 1998.
48. **Wise RA.** Neurobiology of addiction. *Curr Opin Neurobiol* 6: 243–251, 1996.
49. **Zapata P.** Chemosensory activity in the carotid nerve: effects of pharmacological agents. In: *The Carotid Body Chemoreceptors*, edited by González C. Heidelberg: Springer-Verlag, 1997, p. 119–146.